Angewandte Chemie
Eine Zeitschrift der Gesellschaft Deutscher Chemiker

Supporting Information

Identification of RNA Base Pairs and Complete Assignment of Nucleobase Resonances by Proton-Detected Solid-State NMR Spectroscopy at 100 kHz MAS

Philipp Innig Aguion, John Kirkpatrick, Teresa Carlomagno, and Alexander Marchanka**

anie_202107263_sm_miscellaneous_information.pdf

Author Contributions

T.C. Conceptualization: Equal; Data curation: Equal; Funding acquisition: Lead; Supervision: Equal; Writing – original draft: Equal; Writing – review & editing: Lead
P.A. Data curation: Equal; Formal analysis: Equal; Investigation: Equal; Methodology: Equal; Writing – original draft: Equal
J.K. Investigation: Supporting; Writing – review & editing: Equal
A.M. Conceptualization: Equal; Formal analysis: Equal; Investigation: Equal; Methodology: Lead; Supervision: Equal; Writing – original draft: Equal.

SUPPORTING INFORMATION

Table of Contents

Experimental Procedures

Protein expression and purification. The L7Ae protein from *Pf* was expressed and purified through a denaturing purification protocol, as described in detail elsewhere.[1] Briefly, L7Ae was expressed from the pET-M11 expression vector, containing an N-terminal hexa-histidine tag, followed by a TEV (tobacco etch virus) protease cleavage site, in *Escherichia coli* BL21 (DE3) cells using LB medium.[2] Cells were grown at 37 °C and expression was induced at OD_{600} = 0.6–0.8 by addition of 0.6 mM isopropyl-β-D-thiogalactopyranoside (IPTG). Expression was continued for 16–20 hours at 18 °C. Cells were harvested by centrifugation at 4000 g at 4 °C and lysed by sonication in the lysis buffer (50 mM Tris-HCl pH 7.5, 1 M NaCl, 2 mM β-mercaptoethanol (BME), 10 mM imidazole) with the addition of 0.2 mg/mL lysozyme, 40 μg/mL DNAse I and 1x protease inhibitor cocktail (Roche). The centrifuged (45 min, 4 °C, 32000 g) and filtered (0.45 μm) lysate was mixed with 8 M guanidinium chloride (GuHCl) pH 7.5 at a volume ratio of 1:3. The L7Ae protein was then purified by immobilized-metal-ion affinity chromatography (IMAC) with a HisTrap HP 5 mL column (GE Healthcare). The column was equilibrated with denaturing buffer (50 mM Tris-HCl, pH 7.5, 6 M GuHCl, 1 M NaCl, 2 mM BME, 10 mM imidazole); the protein solution was applied to the column and washed with 5 column volumes (CV) of denaturing buffer prior to protein refolding on the column by a 40 CV buffer gradient, which brought the column back into the lysis buffer. L7Ae was eluted with a 0–100 % gradient of elution buffer (50 mM Tris-HCl pH 7.5, 1 M NaCl, 2 mM BME, 300 mM imidazole) over 4 CVs. The tagged L7Ae protein was incubated with TEV protease (1:30 protease:protein ratio) overnight at room temperature in lysis buffer. The cleaved protein was isolated by reverse IMAC using a HisTrap HP column and further purified by size-exclusion chromatography (SEC) with a Superdex75 Increase 10/300 column (GE Healthcare) in SEC buffer (50 mM Tris-HCl pH 7.5, 1 M NaCl, 2 mM BME).

RNA synthesis. Uniformly ^{1}H,^{13}C,^{15}N-labeled 26mer box C/D RNA (5´-GCUGAGCUCGAAAGAGCA-AUGAUGUC-3´) was prepared by *in vitro* transcription with T7 polymerase (produced in house), ^{13}C, ^{15}N labeled NTPs and plasmid DNA template in transcription buffer (40 mM Tris-HCl pH = 8.0, 1 mM spermidine, 10 mM DTT, 0.01 % Triton X-100 and 0.1 % PEG8000).[3] Transcription yields were optimized in 20 μL small-scale reactions in micro-crystallization 96-well plates with varying concentrations of $MgCl_2$ (20 to 50 mM), rNTPs (10 to 40 mM), plasmid DNA (25 to 200 ng/μL) and *in-house* produced T7 polymerase (25 to 100 ng/μL).[3] ^{13}C and ^{15}N labeling was achieved using commercially available ^{13}C,^{15}N-labeled rNTPs (Silantes). Small-scale reactions were incubated for 2 to 3 h at 37 °C and analyzed via analytical polyacrylamide gel electrophoresis (PAGE), using ethidiumbromid staining and UV visualization. The conditions leading to the best RNA yield were used for preparative-scale reactions. Thermostable inorganic pyrophosphatase (TIPP) (NEB) was added to the reaction to remove pyrophosphate. Preparative transcription reactions were stopped after 6 h by addition of EDTA (final concentration 50 mM). The RNA was purified by denaturing 15 % PAGE and extracted from the gel using the 'crush and soak' method in RNA elution buffer (40 mM MOPS pH 6.0, 11 mM EDTA) for 16 h at 4 °C prior to EtOH/NaCl precipitation. The pure RNA was dissolved in water.[1]

Assembly of L7Ae–26mer box C/D RNA complex. The individual components of the complex were tested for RNAse contamination using the RNAseAlert™ Lab Test Kit prior to complex assembly. The L7Ae–26mer box C/D RNA complex was assembled by mixing L7Ae protein and 26mer box C/D RNA in a 1.1:1 molar ratio. The mixture was incubated at 80 °C for 15 min, slowly cooled to room temperature and then purified by SEC on a Superdex75 Increase 10/300 column in RNP buffer (25 mM HEPES pH 7.5, 120 mM NaCl). The pure protein–RNA complex was concentrated to ~20 mg/ml in RNP buffer and subsequently mixed with an equal volume of

precipitation solution (100 mM sodium acetate, 30 % PEG 400 in 100 mM HEPES, pH 7.5 in 100 % H_2O or 50 % D_2O) as described elsewhere.[4–7] The sample was micro-crystallized by slow precipitation using a SpeedVac concentrator at room temperature for ~2 hours. The complex precipitated at approximately half the starting volume. The precipitate was packed into a 0.81-mm MAS ssNMR rotor by centrifugation at 80000 g for 2 h. In total, 800 μg of the L7Ae–26mer box C/D RNA complex were packed into the 0.81-mm rotor, corresponding to ~300 μg of the labeled RNA.

NMR spectroscopy. All NMR experiments were acquired on a Bruker Avance III HD NMR spectrometer operating at a ^{1}H field-strength of 850 MHz and equipped with a 0.81-mm triple-resonance HCN probe developed in the Samoson laboratory (https://www.nmri.eu/).[8] All presented spectra were recorded with samples prepared in 100 % H_2O, except those shown in Fig. 6d and e, which were recorded on a sample prepared in 50 % D_2O. For observation of the NH_2 groups in the 3D (HN)H(H)NH spectrum, we chose to record the spectrum in a buffer containing 50 % D_2O, sacrificing 10–20 % peak intensity in favor of ~20–25 % narrower linewidths, resulting from longer proton coherence lifetimes. However, the quality of the spectrum did not significantly improve compared to the spectrum recorded in 100 % H_2O (shown in Fig. S4).

The final temperature of the assignment experiments was optimized by inspecting 2D ^{1}H-^{15}N HSQCs recorded at temperatures of 260 K, 265 K, 275 K, 280 K and 285 K. The ^{1}H linewidths of a few nucleotides (e.g. G10, A15, A18, A19) became significantly broader at lower temperatures, while other nucleotides (e.g. U3, C7, U20) were unaffected by temperature changes. Conversely, the signal-to-noise ratio of most peaks was worse at higher temperatures (e.g. 280 K and 285 K). Thus, we chose the temperature of 275 K as a compromise between the temperature-dependent linewidths and sensitivity. All spectra for resonance assignment were recorded at a magic-angle spinning rate of 100 kHz.

WALTZ-16[9] decoupling with $\nu = \gamma B_1/2\pi = 10\ \mathrm{kHz}$ was used for ^{1}H decoupling during indirect heteronuclear evolution periods (e.g. ^{13}C, ^{15}N). WALTZ-16 was also used for ^{15}N decoupling during evolution of either ^{1}H or ^{13}C spins, including the direct acquisition time. DIPSI-3[10] decoupling with $\nu = \gamma B_1/2\pi = 20\ \mathrm{kHz}$ was used for ^{13}C decoupling during either ^{1}H or ^{15}N evolution times. The MISSISSIPPI[11] scheme without the homospoil gradient ($\nu = \gamma B_1/2\pi = 40\ \mathrm{kHz}$) was employed to suppress the residual H_2O signal during z-storage of ^{13}C or ^{15}N magnetization.

The shapes, offsets, durations and powers employed for CP transfers are summarized in Table S2. Selective ^{13}C and ^{15}N refocusing pulses from the BURP family[12] were applied to eliminate signals outside the region of interest. The ^{15}N and ^{13}C carrier frequencies are summarized in Table S1.

^{13}C chemical shifts were referenced as described by Morcombe and Zilm.[13] ^{15}N and ^{1}H chemical shifts were referenced indirectly using chemical shift referencing ratios from the work of Markley *et al*.[14] Spectra were processed with NMRPipe[15] and visualized and assigned with CcpNmr Analysis.[16]

SUPPORTING INFORMATION

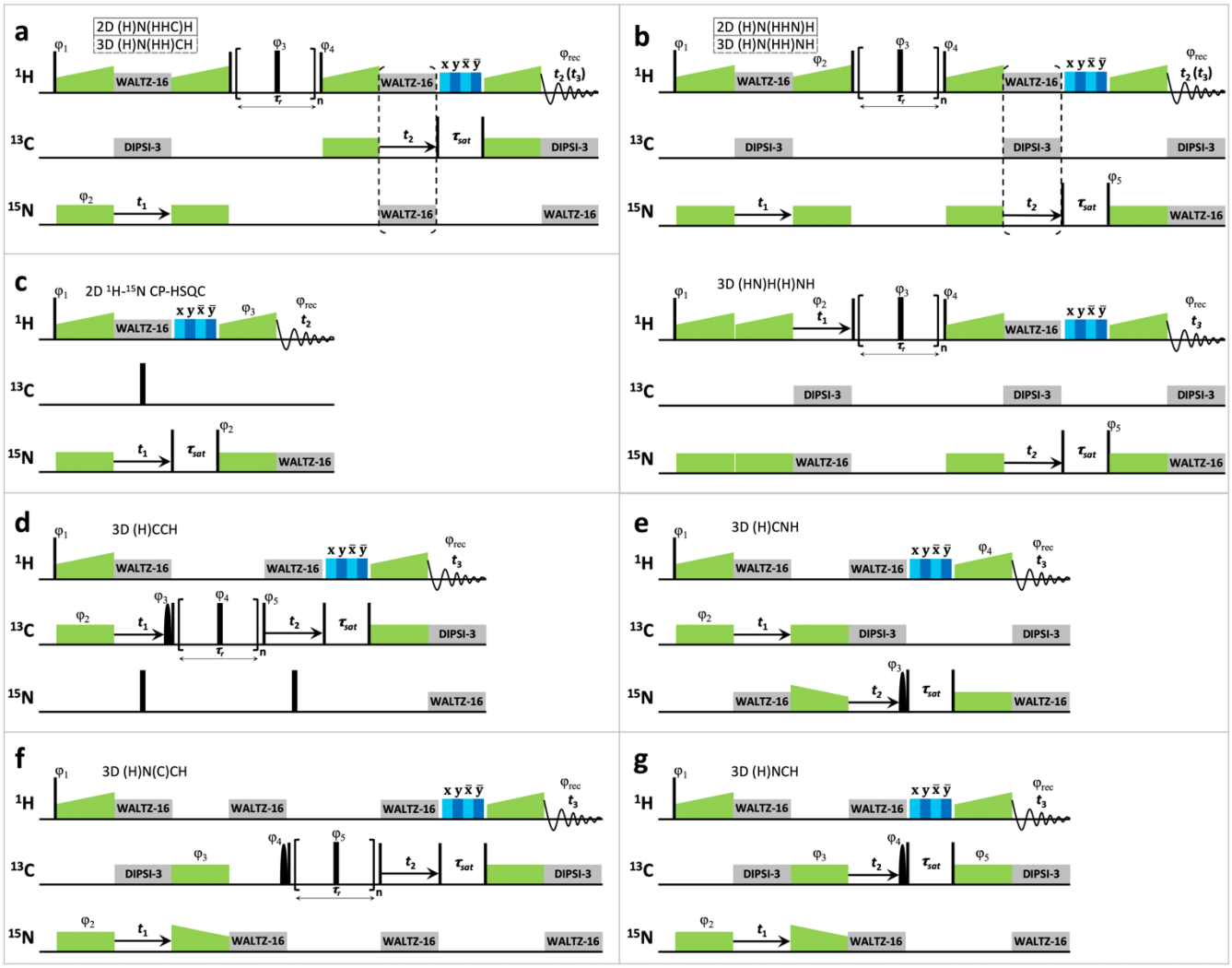

Figure S1. Pulse sequences of all experiments. (**a**) 2D (H)N(HHC)H and 3D (H)N(HH)CH experiments. In the 3D experiment the ^{13}C chemical shifts were recorded during t_2. The phase cycle was φ_1 = y, –y; φ_2 = 2(x), 2(–x); φ_3 = x, y, x, y, y, x, y, x; φ_4 = 4(y), 4(–y); φ_{rec} = x, –x, –x, x, –x, x, x, –x. (**b**) 2D (H)N(HHN)H, 3D (H)N(HH)NH and 3D (HN)H(H)NH experiments. In the 3D experiments the ^{15}N chemical shifts were recorded during t_2. In t_1 either ^{15}N (3D (H)N(HH)NH) or ^{1}H (3D (HN)H(H)NH) chemical shifts were recorded. The phase cycle was φ_1 = y, –y; φ_2 = 2(y), 2(–y); φ_3 = x, y, x, y, y, x, y, x; φ_4 = 4(y), 4(–y); φ_5 = 8(y), 8(–y); φ_{rec} = x, –x, –x, x, –x, x, x, –x, –x, x, x, –x, x, –x, –x, x. (**c**) 2D ^{1}H-^{15}N CP-HSQC experiment. The phase cycle was φ_1 = y, –y; φ_2 = 2(x), 2(–x); φ_3 = 4(y), 4(–y) φ_{rec} = y, –y, –y, y, –y, y, y, –y. (**d**) Base-selective 3D (H)CCH experiment. The phase cycle was φ_1 = 2(y), 2(–y); φ_2 = y, –y; φ_3 = 8(x), 8(y); φ_4 = x, y, x, y, y, x, y, x; φ_5 = 4(x), 4(–x); φ_{rec} = x, –x, –x, x, –x, x, x, –x, –x, x, x, –x, x, –x, –x, x. (**e**) Amino- and imino-selective 3D (H)CNH experiment. The phase cycle was φ_1 = y, –y; φ_2 = 2(y), 2(–y); φ_3 = 4(x), 4(y), 4(–x), 4(–y); φ_4 = 16(y), 16(–y); φ_{rec} = 2(–y, y, y, –y, y, –y, –y, y), 2(y, –y, –y, y, –y, y, y, –y). (**f**) Base-selective 3D (H)N(C)CH experiment. The phase cycle was φ_1 = 2(y), 2(–y); φ_2 = y, –y; φ_3 = 2(x), 2(–x); φ_4 = 4(x), 4(y); φ_5 = x, y, x, y, y, x, y, x; φ_{rec} = x, –x, –x, x, –x, x, x, –x. (**g**) Base-selective (H)NCH experiment. The phase cycle was φ_1 = 4(y), 4(–y); φ_2 = y, –y; φ_3 = 2(x), 2(–x); φ_4 = 8(x), 8(y); φ_5 = 8(y), 8(–y); φ_{rec} = 2(–y, y, y, –y, y, –y, –y, y), 2(y, –y, –y, y, –y, y, y, –y).

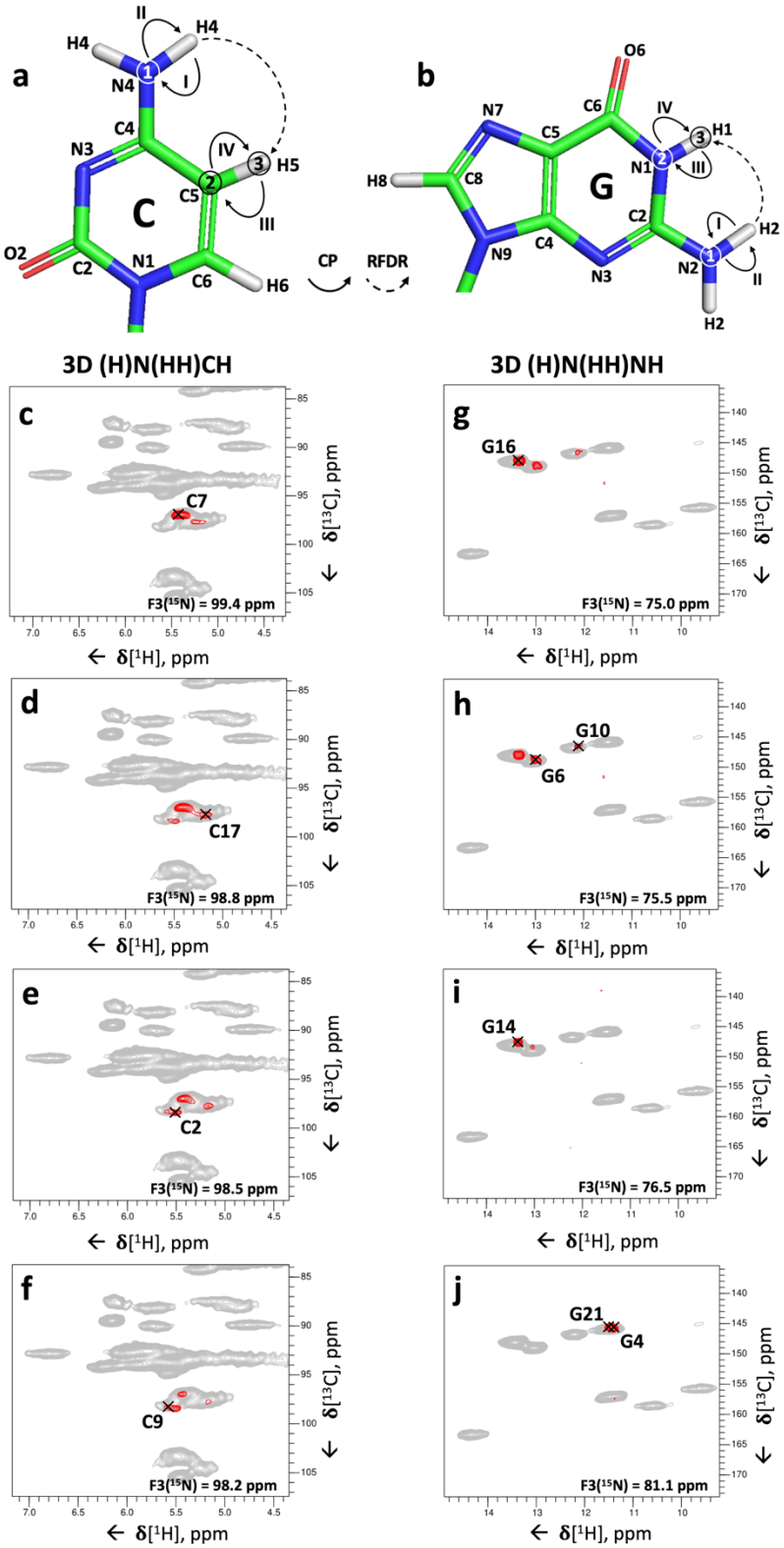

Figure S2. 3D (H)N(HH)CH and 3D (H)N(HH)NH experiments for the assignment of nucleobase amino resonances. (**a**) Magnetization transfer scheme of the 3D (H)N(HH)CH experiment shown for cytidine. (**b**) Magnetization transfer scheme for the N2–N1–H1 correlations of guanosines in the 3D (H)N(HH)NH experiment. Encircled numbers indicate the chemical-shift evolution times (t_1–t_3) corresponding to the three spectral dimensions; roman numerals I, II, III and IV indicate the first, second, third and fourth CP transfer periods, respectively. (**c-f**) Representative 2D ^{1}H -^{13}C planes from the 3D (H)N(HH)CH spectrum showing cytidine N4–C5–H5 correlations for the nucleotides C7 (**c**), C17 (**d**), C2 (**e**) and C9 (**f**). The ^{1}H-^{1}H RFDR mixing time was 0.48 ms. (**g-j**) Representative 2D ^{1}H-^{15}N planes extracted from the 3D (H)N(HH)NH spectrum showing guanosine N2–N1–H1 correlations for the nucleotides G16 (**g**), G6 and G10 (**h**), G14 (**i**), G21 and G4 (**j**). The ^{1}H-^{1}H RFDR mixing time was 0.48 ms. For reference, in panels (c-f) the red contours of the 3D (H)N(HH)CH spectrum are overlaid on the 2D ^{1}H-^{13}C CP-HSQC spectrum (in grey) tailored for the ribose/C5-H5 spectral region; in panels (g-j) the red contours of the 3D (H)N(HH)NH spectrum are overlaid on the 2D ^{1}H-^{15}N CP-HSQC spectrum (in grey). The pulse sequences and phase cycles are given in Fig. S1a and b.

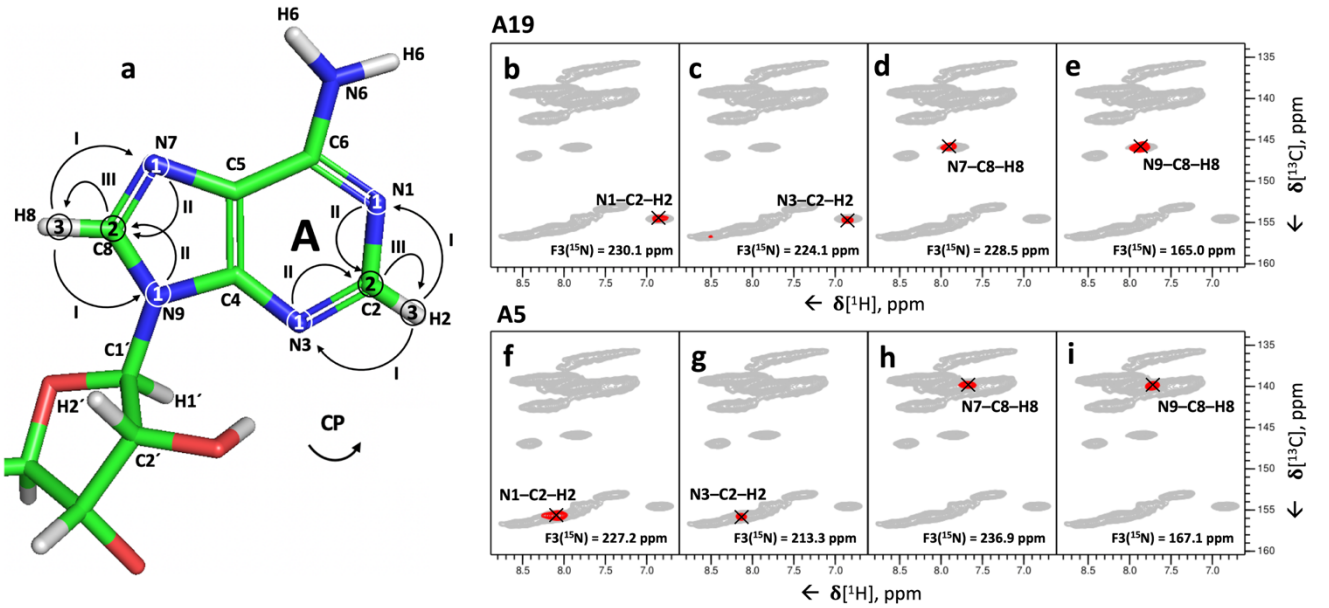

Figure S3. Assignment of non-protonated nucleobase nitrogen chemical shifts by the 3D (H)NCH experiment. (**a**) Magnetization transfer scheme of the 3D (H)NCH experiment shown for adenosine as an example. Encircled numbers indicate the chemical-shift evolution times (t_1–t_3) corresponding to the three spectral dimensions; roman numerals I, II and III indicate the first (5 ms), second (8 ms) and third (0.25 ms) CP transfer periods. (**b-i**) Representative 2D ^{1}H -^{13}C planes extracted from the 3D (H)NCH spectrum showing the A19-N1–C2–H2 cross-peak (**b**), the A19-N3–C2–H2 cross-peak (**c**), the A19-N7–C8–H8 cross-peak **(d**), the A19-N9–C8–H8 cross-peak (**e**), the A5-N1–C2–H2 cross-peak (**f**), the A5-N3–C2–H2 cross-peak (**g**), the A5-N7–C8–H8 cross-peak **(h**), the A5-N9–C8–H8 cross-peak (**i**). The pulse sequence and phase cycle of the 3D (H)NCH experiment are given in Fig. S1g. For reference, in panels (b-i) the red contours of the 3D(H)N(C)CH spectrum are overlaid on the 2D ^{1}H-^{13}C CP-HSQC spectrum (in grey) tailored for nucleobase resonances.

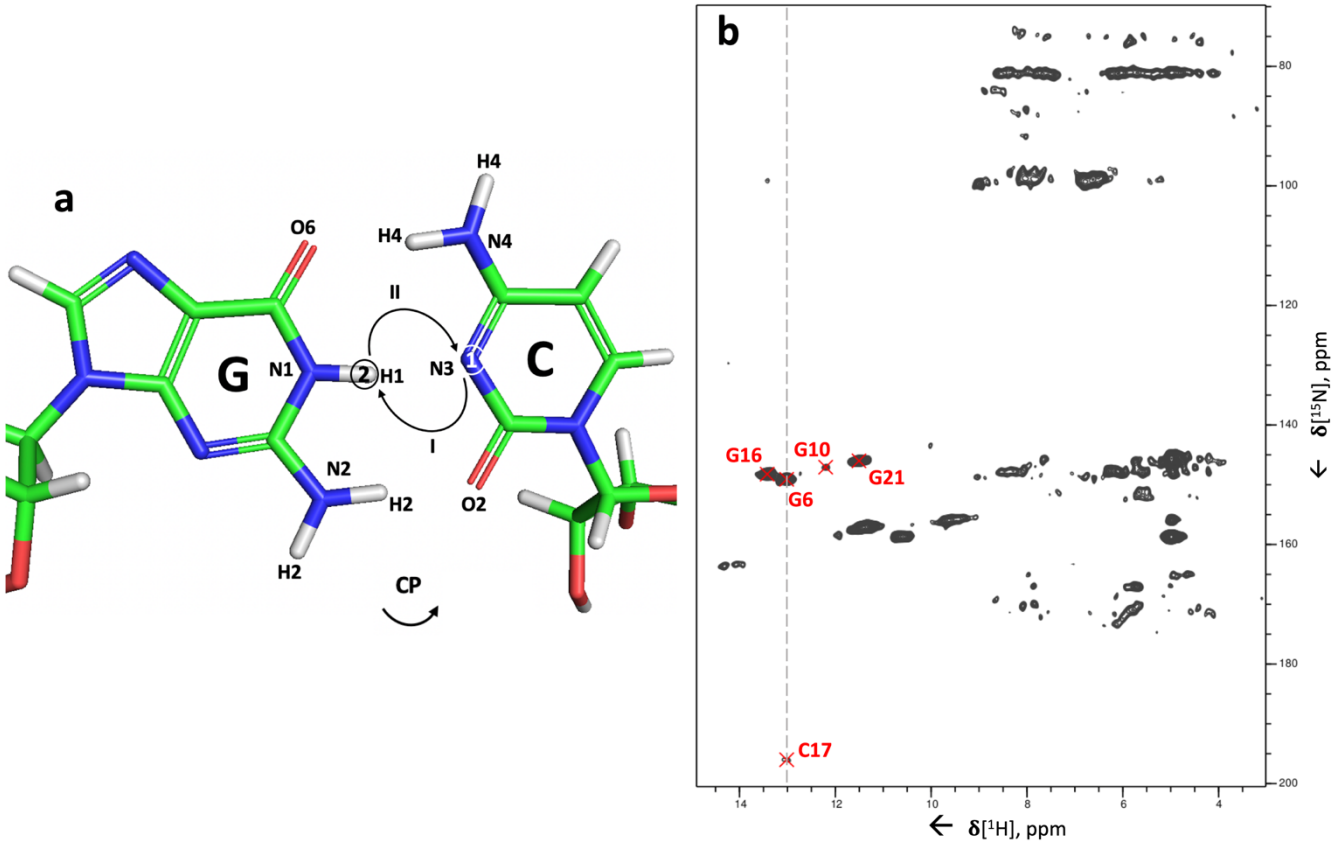

Figure S4. Assignment of C-N3 resonances by the 2D long-range ^{1}H-^{15}N CP-HSQC experiment. (**a**) Magnetization transfer scheme of the 2D ^{1}H-^{15}N CP-HSQC experiment shown for inter-strand G-H1–C-N3 correlations. Encircled numbers indicate the chemical-shift evolution times (t_1 & t_2) corresponding to the two spectral dimensions; roman numerals I and II indicate the first and second CP transfer times (both 8 ms). (**b**) 2D ^{1}H-^{15}N CP-HSQC experiment with 8 ms-long ^{1}H-^{15}N/^{15}N-^{1}H CP transfer times. The pulse sequence and phase cycle of the 2D ^{1}H-^{15}N CP-HSQC experiment are given in Fig. S1c.

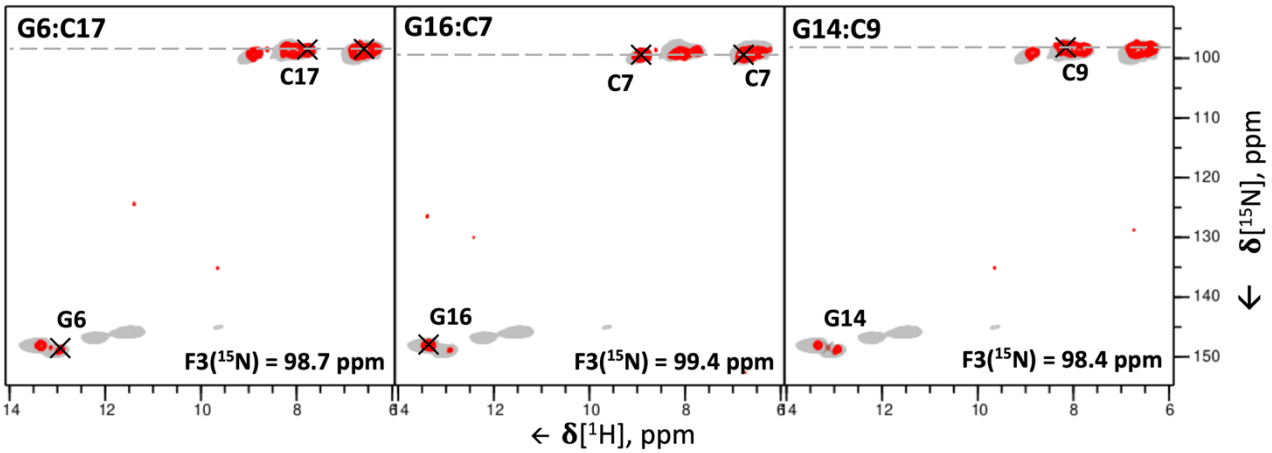

Figure S5. Detection of G:C base pairs by the 3D (H)N(HH)NH experiment. Representative 2D ^{1}H-^{15}N planes extracted from the 3D (H)N(HH)NH spectrum showing C-N4–G-N1–H1 cross-peaks for the base pairs G6:C17, C7:G16 and C9:G14. The pulse sequence and phase cycle of the 3D (H)N(HH)NH experiment are given in Fig. S1b. For reference, the red contours of the 3D (H)N(HH)NH spectrum are overlaid on the 2D ^{15}N-^{1}H CP-HSQC spectrum (in grey).

SUPPORTING INFORMATION

Table S1. Acquisition parameters and evolution times of all spectra.

Spectrum ↓	Indirect evolution times, ms					Carrier frequencies, ppm			Acq, ms	Spectral widths, kHz (ppm)						RFDR mixing time, ms	Scans per point	Exp. time, h
Dimensions →	^{1}H	^{13}C	^{13}C	^{15}N	^{15}N	^{1}H	^{13}C	^{15}N	^{1}H	^{1}H	^{13}C	^{13}C	^{15}N	^{15}N	^{1}H acq			
2D ^{1}H-^{13}C HSQC ribose-selective	-	6.0	-	-	-	7.1	70	170	12.8	-	21 (100)	-	-	-	40 (47)	-	32	5.1
2D ^{1}H-^{13}C HSQC base-selective	-	7.5	-	-	-	7.1	140	170	12.8	-	13 (60)	-	-	-	40 (47)	-	64	7.6
2D ^{1}H-^{15}N HSQC	-	-	-	9.7	-	7.1	140	117.5	12.8	-	-	-	10 (120)	-	40 (47)	-	64	7.9
2D ^{1}H-^{15}N HSQC, 50 % D_2O	-	-	-	9.7	-	7.1	140	117.5	12.8	-	-	-	10 (120)	-	40 (47)	-	64	6.2
2D ^{1}H-^{15}N HSQC, long-range	-	-	-	8.2	-	7.1	140	135	12.8	-	-	-	12 (140)	-	40 (47)	-	138	16
2D (H)N(HHC)H	-	-	-	5.8	-	7.1	160	160	12.8	-	-	-	13.8 (160)	-	40 (47)	0.40	128	12
2D (H)N(HHN)H	-	-	-	6.2	-	7.1	140	117.5	12.8	-	-	-	10 (120)	-	40 (47)	0.48	192	15
3D (H)CCH base-selective	-	3.7	3.7	-	-	7.1	135	170	10.0	-	17 (80)	17 (80)	-	-	40 (47)	8	16	137
3D (H)CNH amino-selective	-	4.4	-	3.7	-	7.1	155	80	12.8	-	11 (50)	-	4.3 (50)	-	40 (47)	-	32	61
3D (H)CNH imino-selective	-	5.6	-	5.4	-	7.1	160	154	12.8	-	4.3 (20)	-	2.2 (26)	-	40 (47)	-	64	36
3D (H)N(C)CH base-selective	-	2.9	-	3.7	-	7.1	134	120	6.4	-	6.8 (32)	-	8.6 (100)	-	40 (47)	14	64	80
3D H(NC)CH base-selective	2.1	2.9	-	-	-	7.1	130	120	6.4	9.4 (11)	8.6 (40)	-	-	-	40 (47)	14	64	62
3D (H)NCH base-selective	-	5.0	-	5.9	-	7.1	149	190	12.8	-	6.4 (30)	-	9.5 (110)	-	40 (47)	-	16	56
3D (H)N(HH)CH, short RFDR	-	4.5	-	5.6	-	7.1	85	120	12.8	-	11 (50)	-	8.6 (100)	-	40 (47)	0.48	16	91
3D (H)N(HH)CH, long RFDR	-	4.5	-	4.5	-	7.1	85	120	12.8	-	11 (50)	-	8.6 (100)	-	40 (47)	0.96	24	111
3D (H)N(HH)NH	-	-	-	6.0	6.0	7.1	140	117.5	12.8	-	-	-	8.6 (100)	8.6 (100)	40 (47)	0.48	16	107
3D (HN)H(H)NH	3.4	-	-	5.0	-	10.0	140	117.5	7.5	9.4 (11)	-	-	8.6 (100)	-	40 (47)	0.48	32	85

Table S2. Summary of cross-polarization conditions.

Spectrum ↓	Transfer	Contact time, ms	Type	Max (average) RF strength, kHz		RF pulse shape	
				Starting nucleus	Ending nucleus	Starting nucleus	Ending nucleus
2D ^{1}H-^{13}C HSQC ribose-selective	^{1}H ⟶ ^{13}C	0.35	DQ(n=1)	73.6	30.2	Linear ramp up ±30%	Rectangle
	^{13}C ⟶ ^{1}H	0.20	ZQ(n=1)	30.2	129.4	Rectangle	Linear ramp up ±30%
2D ^{1}H-^{13}C HSQC base-selective	^{1}H ⟶ ^{13}C	0.35	DQ(n=1)	73.6	30.2	Linear ramp up ±30%	Rectangle
	^{13}C ⟶ ^{1}H	0.20	ZQ(n=1)	30.2	129.4	Rectangle	Linear ramp up ±30%
2D ^{1}H-^{15}N HSQC	^{1}H ⟶ ^{15}N	0.60	DQ(n=1)	80.0	25.2	Linear ramp up ±30%	Rectangle
	^{15}N ⟶ ^{1}H	0.80	ZQ(n=1)	25.2	126.1	Rectangle	Linear ramp up ±30%
2D ^{1}H-^{15}N HSQC, 50 % D_2O	^{1}H ⟶ ^{15}N	0.80	DQ(n=1)	78.6	25.2	Linear ramp up ±30%	Rectangle
	^{15}N ⟶ ^{1}H	0.65	ZQ(n=1)	25.2	127.5	Rectangle	Linear ramp up ±30%
2D ^{1}H-^{15}N HSQC, long-range	^{1}H ⟶ ^{15}N	8.0	DQ(n=1)	86.2	25.2	Linear ramp up ±30%	Rectangle
	^{15}N ⟶ ^{1}H	8.0	ZQ(n=1)	25.2	127.5	Rectangle	Linear ramp up ±30%
2D (H)N(HHC)H	^{1}H ⟶ ^{15}N	0.80	DQ(n=1)	81.0	25.2	Linear ramp up ±30%	Rectangle
	^{15}N ⟶ ^{1}H	0.60	ZQ(n=1)	25.2	119.8	Rectangle	Linear ramp up ±30%
	^{1}H ⟶ ^{13}C	0.35	DQ(n=1)	73.0	30.2	Linear ramp up ±30%	Rectangle
	^{13}C ⟶ ^{1}H	0.45	ZQ(n=1)	30.2	128.4	Rectangle	Linear ramp up ±30%
2D (H)N(HHN)H	^{1}H ⟶ ^{15}N	0.60	DQ(n=1)	81.2	25.2	Linear ramp up ±30%	Rectangle
	^{15}N ⟶ ^{1}H	0.80	ZQ(n=1)	25.2	135.5	Rectangle	Linear ramp up ±30%
3D (H)CCH base-selective	^{1}H ⟶ ^{13}C	3.0	DQ(n=1)	73.0	30.2	Linear ramp up ±30%	Rectangle
	^{13}C ⟶ ^{1}H	0.50	ZQ(n=1)	30.2	128.4	Rectangle	Linear ramp up ±30%
3D (H)CNH amino-selective	^{1}H ⟶ ^{13}C	3.0	DQ(n=1)	73.0	20.0	Linear ramp up ±30%	Rectangle
	^{13}C ⟶ ^{15}N	7.0	DQ(n=1)	62.4	39.1	Rectangle	Tangential down ±10%
	^{15}N ⟶ ^{1}H	1.0	ZQ(n=1)	25.2	119.8	Rectangle	Linear ramp up ±30%
3D (H)CNH imino-selective	^{1}H ⟶ ^{13}C	3.0	DQ(n=1)	73.0	20.0	Linear ramp up ±30%	Rectangle
	^{13}C ⟶ ^{15}N	7.0	DQ(n=1)	62.4	39.1	Rectangle	Tangential down ±10%
	^{15}N ⟶ ^{1}H	1.0	ZQ(n=1)	25.2	119.8	Rectangle	Linear ramp up ±30%
3D (H)N(C)CH base-selective	^{1}H ⟶ ^{15}N	1.0	DQ(n=1)	81.0	25.2	Linear ramp up ±30%	Rectangle
	^{15}N ⟶ ^{13}C	10.0	DQ(n=1)	39.9	62.4	Tangential down ±10%	Rectangle
	^{13}C ⟶ ^{1}H	0.4	ZQ(n=1)	30.2	128.4	Rectangle	Linear ramp up ±30%
3D H(NC)CH base-selective	^{1}H ⟶ ^{15}N	0.60	DQ(n=1)	81.2	25.2	Linear ramp up ±30%	Rectangle
	^{15}N ⟶ ^{13}C	8.0	DQ(n=1)	40.8	62.4	Tangential down ±10%	Rectangle

	$^{13}C \longrightarrow {}^{1}H$	0.20	ZQ(n=1)	30.2	128.7	Rectangle	Linear ramp up ±30%
3D (H)NCH base-selective	$^{1}H \longrightarrow {}^{15}N$	5.0	DQ(n=1)	73.0	25.2	Linear ramp up ±30%	Rectangle
	$^{15}N \longrightarrow {}^{13}C$	8.0	DQ(n=1)	40.8	60.1	Tangential down ±10%	Rectangle
	$^{13}C \longrightarrow {}^{1}H$	0.25	ZQ(n=1)	29.5	119.8	Rectangle	Linear ramp up ±30%
3D (H)N(HH)CH, short RFDR	$^{1}H \longrightarrow {}^{15}N$	0.80	DQ(n=1)	79.2	25.2	Linear ramp up ±30%	Rectangle
	$^{15}N \longrightarrow {}^{1}H$	0.60	ZQ(n=1)	25.2	119.8	Rectangle	Linear ramp up ±30%
	$^{1}H \longrightarrow {}^{13}C$	0.35	DQ(n=1)	73.0	30.2	Linear ramp up ±30%	Rectangle
	$^{13}C \longrightarrow {}^{1}H$	0.45	ZQ(n=1)	30.2	128.4	Rectangle	Linear ramp up ±30%
3D (H)N(HH)CH, long RFDR	$^{1}H \longrightarrow {}^{15}N$	0.80	DQ(n=1)	79.2	25.2	Linear ramp up ±30%	Rectangle
	$^{15}N \longrightarrow {}^{1}H$	0.60	ZQ(n=1)	25.2	119.8	Rectangle	Linear ramp up ±30%
	$^{1}H \longrightarrow {}^{13}C$	0.35	DQ(n=1)	73.0	30.2	Linear ramp up ±30%	Rectangle
	$^{13}C \longrightarrow {}^{1}H$	0.45	ZQ(n=1)	30.2	128.4	Rectangle	Linear ramp up ±30%
3D (H)N(HH)NH	$^{1}H \longrightarrow {}^{15}N$	0.80	DQ(n=1)	79.2	25.2	Linear ramp up ±30%	Rectangle
	$^{15}N \longrightarrow {}^{1}H$	0.80	ZQ(n=1)	25.2	125.5	Rectangle	Linear ramp up ±30%
3D (HN)H(H)NH	$^{1}H \longrightarrow {}^{15}N$	0.45	DQ(n=1)	78.6	25.2	Linear ramp up ±30%	Rectangle
	$^{15}N \longrightarrow {}^{1}H$	0.65	ZQ(n=1)	25.2	127.5	Rectangle	Linear ramp up ±30%

SUPPORTING INFORMATION

Table S3. Fourier processing parameters of all spectra.

Spectrum ↓	**Digital resolution**						**Window function**					
Dimensions →	^{1}H	^{13}C	^{13}C	^{15}N	^{15}N	^{1}H acq	^{1}H	^{13}C	^{13}C	^{15}N	^{15}N	^{1}H acq
2D ^{1}H-^{13}C HSQC ribose-selective	-	1024	-	-	-	8192	-	QSINE2	-	-	-	QSINE2
2D ^{1}H-^{13}C HSQC base-selective	-	1024	-	-	-	8192	-	QSINE2	-	-	-	QSINE2
2D ^{1}H-^{15}N HSQC	-	-	-	1024	-	4096	-	-	-	QSINE2	-	QSINE2
2D ^{1}H-^{15}N HSQC, 50 % D_2O	-	-	-	1024	-	4096	-	-	-	QSINE2	-	QSINE2
2D ^{1}H-^{15}N HSQC, long-range	-	-	-	1024	-	4096	-	-	-	QSINE2	-	QSINE2
2D (H)N(HHC)H	-	-	-	1024	-	8192	-	-	-	QSINE2		GM -70Hz/0.2
2D (H)N(HHN)H	-	-	-	1024	-	4096	-	-	-	QSINE2	-	GM -80Hz/0.2
3D (H)CCH base-selective	-	256	256	-	-	4096	-	QSINE2	QSINE2	-	-	GM -40Hz/0.2
3D (H)CNH amino-selective	-	256	-	128	-	4096	-	QSINE2	-	GM -30Hz/0.2	-	GM -40Hz/0.2
3D (H)CNH imino-selective	-	256	-	128	-	4096	-	QSINE2	-	GM -30Hz/0.2	-	GM -40Hz/0.2
3D (H)N(C)CH base-selective	-	256	128	256	-	4096	-	GM -30Hz/0.2	-	QSINE2	-	GM -40Hz/0.2
3D H(NC)CH base-tuned	128	256	-	-	-	4096	QSINE 2	GM -30Hz/0.2	-	-	-	GM -40Hz/0.2
3D (H)NCH base-selective	-	128	-	256	-	4096	-	QSINE2	-	GM -30Hz/0.2	-	GM -70Hz/0.2
3D (H)N(HH)CH, short RFDR	-	256	-	256	-	4096	-	GM -30Hz/0.2	-	QSINE2	-	GM -40Hz/0.2
3D (H)N(HH)CH, long RFDR	-	256	-	256	-	4096	-	GM -30Hz/0.2	-	QSINE2	-	GM -40Hz/0.2
3D (H)N(HH)NH	-	-	-	256	256	4096	-	-	-	GM -30Hz/0.2	QSINE2	GM -40Hz/0.2
3D (HN)H(H)NH	128	-	-	256	-	8192	QSINE 2	-	-	GM -50Hz/0.2	-	GM -70Hz/0.2

SUPPORTING INFORMATION

Table S4. Inter-strand and intra-residue distances in trans-Hoogsteen/sugar-edge G:A base pairs derived from published structures (Ahmed *et al.*, 2020[1] PDB entry 6TPH; Correll *et al.*, 1997[17] PDB entry 354D; Cate *et al.*, 1996[18] PDB entry 1GID).

atom distance in trans-Hoogsteen/sugar edge G:A base pairs, Å				
	Inter-strand distance		**Intra-residue distance**	
G:A base pair	**G-H1´–A-H6**	**G-H2–A-H8**	**G-H1´–H2**	**A-H6–H8**
Ahmed *et al.*, 2020[1] 4G:22A	2.6	3.5	4.2	5.1
Ahmed *et al.*, 2020[1] 5A:21G	2.3	3.0	4.5	5.1
Correll *et al.*, 1997[17] 72G:104A	2.4	3.3	4.6	4.9
Cate *et al.*, 1996[18] 150G:153A	2.4	2.3	4.5	4.9
Cate *et al.*, 1996[18] 140A:163G	2.2	3.4	4.5	4.9
Cate *et al.*, 1996[18] 139A:164G	2.4	2.9	4.5	4.9
Average	**2.4**	**3.1**	**4.5**	**5.0**
Standard deviation	0.1	0.4	0.1	0.1

SUPPORTING INFORMATION

Table S5. Isotropic chemical shifts of the 26mer box C/D RNA in the L7Ae–box C/D RNA complex, obtained in this work and our previous study[19] using ^{1}H-detection. Chemical shifts measured here are highlighted in light-blue. Unassigned spins are indicated with a dash and ambiguous assignments are marked by with an asterisk.

	Isotropic chemical shifts, ppm																											
	C1'	C2	C2'	C3'	C4	C4'	C5	C5'	C6	C8	H1	H1'	H2	H2'	H3	H3'	H4	H4'	H5	H5´	H6	H8	N1	N2	N3	N4	N6	N7	N9
C2	-	-	-	-	168.2	-	98.2	-	140.7			-		-		-	8.0	-	5.5	-	7.8		151.8		-	98.5			
U3	94.9	154.3	75.6	71.7	166.2	83.0	104.6	64.0	140.1			5.6		4.2	11.4	4.2		4.3	5.3	4.2/4.4	7.4		145.2		157.0				
G4	90.0	155.9	75.9	79.5	-	88.2	-	67.8	160.6	139.2	11.3	5.7	5.5/7.7	5.0		4.9		4.9		4.0/4.4		8.1	145.7	81.1	-			-	166.9
A5	88.2	155.8	78.5	79.9	-	83.5	121.1	70.3	157.3	139.9		5.7	8.1	4.5		4.9		4.9		4.2/4.4	6.1/8.5*	7.7	227.2		213.5		81.1	236.9	167.2
G6	92.7	157.9	76.0	77.2	152.4	83.5	-	70.9	161.9	139.0	13.0	6.8	9.0/9.3	4.9		4.7		5.0		4.5/4.8		8.3	149.0	75.5	-			-	170.9
C7	93.8	159.1	75.3	72.1	168.7	81.9	96.9	64.3	142.5			6.0		4.5		4.6	6.8/8.9	4.5	5.4	4.2/4.7	8.4		152.4		-	99.4			
U8	93.7	153.0	-	71.8	169.4	-	103.2	-	142.7			5.6		-	14.3	4.7		-	5.5	-	8.3		147.9		163.3				
C9	93.7	158.6	-	-	168.3	-	98.0	-	140.2			5.7		-		-	6.5/8.2	-	5.6	-	7.4		152.1		-	98.2			
G10	93.9	155.9	75.7	-	157.3	-	120.5	-	161.6	136.2	12.2	5.7	6.4/7.0	4.5		-		-		-		7.6	146.7	75.7	-			-	171.2
G14	-	157.4	-	-	-	-	-	-	161.6	137.4	13.3	-	6.7/8.6	-		-		-		-		8.0	148.1	-	-			-	-
A15	92.7	153.2	75.5	72.2	-	81.6	-	64.2	157.9	139.7		6.0	7.4	4.5		4.7		4.6		3.9/4.6	7.1	7.9	222.2		-		82.6	-	171.7
G16	92.5	157.3	75.4	72.1	-	81.6	-	64.3	161.8	136.4	13.4	5.8	7.2/7.7	4.5		-		4.5		4.1/4.6		7.8	148.2	75.1	-			-	171.3
C17	93.5	158.5	75.6	71.7	168.1	81.5	97.6	64.4	139.5			5.6		4.7		4.5	6.6/7.8	4.5	5.2	4.5	7.4		150.9		197.0	98.8			
A18	94.1	156.7	76.6	72.6	-	81.6	118.8	64.6	158.0	138.9		6.3	8.4	4.1		4.8		4.8		4.4/4.6	6.8	8.1	-		-		79.7	231.5	173.2
A19	89.8	154.6	72.2	78.5	150.8	85.1	121.8	67.3	156.5	146.0		4.7	6.9	4.8		4.6		3.4		3.9/4.4	5.9	7.9	230.2		224.0		76.0	228.5	164.9
U20	89.4	154.3	75.3	80.5	168.4	84.2	105.4	69.5	147.0			6.2		4.8	10.6	4.5		5.3	5.5	4.0/4.1	8.5		147.6		158.5				
G21	87.4	156.0	77.5	80.0	-	87.4	117.9	68.1	160.5	139.2	11.5	6.1	5.3/7.6	5.3		5.0		5.2		4.5		8.4	145.8	81.1	-			-	168.7
A22	92.4	156.6	75.8	72.3	-	82.9	118.6	65.8	157.4	140.1		5.8	8.6	5.0		4.6		4.8		4.2/4.6	6.1/8.5*	7.9	223.4		-		81.2	231.7	170.3
U23	93.0	151.2	74.6	72.3	168.0	82.4	103.7	62.9	140.5			4.9		4.4	9.6	4.5		4.4	5.4	4.1/4.6	7.6		145.0		155.9				

References

[1] M. Ahmed, A. Marchanka, T. Carlomagno, *Angew. Chem. Int. Ed.* **2020**, *59*, 6866–6873.
[2] A. Lapinaite, B. Simon, L. Skjaerven, M. Rakwalska-Bange, F. Gabel, T. Carlomagno, *Nature* **2013**, *502*, 519–523.
[3] A. Marchanka, T. Carlomagno, *Methods Enzymol.* **2019**, 615, 333-371.
[4] A. Marchanka, B. Simon, T. Carlomagno, *Angew. Chem. Int. Ed.* **2013**, *52*, 9996–10001.
[5] A. Marchanka, B. Simon, G. Althoff-Ospelt, T. Carlomagno, *Nat. Commun.* **2015**, *6*, DOI 10.1038/ncomms8024.
[6] S. Jehle, M. Falb, J. P. Kirkpatrick, H. Oschkinat, B. J. Van Rossum, G. Althoff, T. Carlomagno, *J. Am. Chem. Soc.* **2010**, *132*, 3842–3846.
[7] S. Asami, M. Rakwalska-Bange, T. Carlomagno, B. Reif, *Angew. Chem. Int. Ed.* **2013**, *52*, 2345–2349.
[8] V. Agarwal, S. Penzel, K. Szekely, R. Cadalbert, E. Testori, A. Oss, J. Past, A. Samoson, M. Ernst, A. Böckmann, B. H. Meier, *Angew. Chem. Int. Ed.* **2014**, *53*, 12253–12256.
[9] A. J. Shaka, J. Keeler, T. Frenkiel, R. Freeman, *J. Magn. Reson.* **1983**, *52*, 335–338.
[10] A. J. Shaka, C. J. Lee, A. Pines, *J. Magn. Reson.* **1988**, *77*, 274–293.
[11] D. H. Zhou, C. M. Rienstra, *J. Magn. Reson.* **2008**, *192*, 167–172.
[12] Y. Li, B. J. Wylie, C. M. Rienstra, *J. Magn. Reson.* **2006**, *179*, 206–216.
[13] C. R. Morcombe, K. W. Zilm, *J. Magn. Reson.* **2003**, *162*, 479–486.
[14] J. L. Markley, A. Bax, Y. Arata, C. W. Hilbers, R. Kaptein, B. D. Sykes, P. E. Wright, K. Wüthrich, *J. Mol. Biol.* **1998**, *280*, 933–952.
[15] F. Delaglio, S. Grzesiek, G. W. Vuister, G. Zhu, J. Pfeifer, A. Bax, *J. Biomol. NMR* **1995**, *6*, 277–293.
[16] W. F. Vranken, W. Boucher, T. J. Stevens, R. H. Fogh, A. Pajon, M. Llinas, E. L. Ulrich, J. L. Markley, J. Ionides, E. D. Laue, *Proteins: Struct., Funct., Bioinf.* **2005**, *59*, 687–696.
[17] C. C. Correll, B. Freeborn, P. B. Moore, T. A. Steitz, *Cell* **1997**, *91*, 705–712.
[18] J. H. Cate, E. A. Doherty, J. A. Doudna, *Protein Eng.* **1997**, *10*, 41.
[19] A. Marchanka, J. Stanek, G. Pintacuda, T. Carlomagno, *Chem. Commun.* **2018**, *54*, 8972–8975.

Author Contributions

PIA performed experiments, analysed data and wrote the paper; JK assisted in the experiments and revised the manuscript; TC designed the project, acquired funds, supervised the project and wrote the manuscript; AM designed the project, performed experiments, supervised the project and wrote the manuscript.